Effects of polarization mode coupling and superposition in a whispering-gallery microresonator

A. T. Rosenberger*
Department of Physics, Oklahoma State University, Stillwater, OK 74078-3072

ABSTRACT

The throughput of a single fiber-coupled whispering-gallery microresonator, such as a fused-silica microsphere, can exhibit induced transparency or absorption, leading to pulse delay or advancement, through the interaction of two coresonant orthogonally polarized whispering-gallery modes having very different quality factors (Q). There are two ways by which these behaviors may be realized. The first method, coupled-mode induced transparency and absorption (CMIT, CMIA), relies on intracavity cross-polarization coupling when only one mode is driven. The second method, coresonant polarization induced transparency and absorption (CPIT, CPIA), uses a simple superposition of orthogonal throughputs (in the absence of intracavity cross-polarization mode coupling) when the two modes are simultaneously driven. In both cases, the throughput behavior is observed on the same polarization component as that of the linearly polarized input. The pulse delay or advancement can be enhanced by taking advantage of the multimode capability of the tapered-fiber coupler, an advantage that is not available to free-space-beam-driven ring resonators. Some predictions of a numerical model for this enhancement, which assumes experimentally realistic conditions, are presented here.

Keywords: whispering-gallery modes, microresonator, slow light, fast light, multimode fiber coupler

1. INTRODUCTION

Induced transparency and absorption are of interest because, in general, induced transparency is accompanied by a spectral region of strong normal dispersion and the possibility of slow light (pulse delay); similarly, induced absorption is often accompanied by strong anomalous dispersion and fast light (pulse advancement). The canonical examples of these phenomena are electromagnetically induced transparency and absorption (EIT, EIA), which illustrate how useful these effects can be.[1]

Another manifestation of induced transparency and absorption occurs in coupled optical resonators. For example, sub-millimeter dielectric disks, cylinders, spheres, and toroids support whispering-gallery modes (WGMs) in which light circulates around the perimeter by total internal reflection. Modes of two different microresonators can couple evanescently if the resonators are almost in contact. This leads to, for example, coupled-resonator induced transparency (CRIT).[2,3] In these systems, coupled-resonator induced absorption (CRIA) has also been observed.[3]

Modes of a single WGM microresonator can also interact. Mode splitting due to backscatter-induced coupling of counterpropagating modes has been observed and studied in detail.[4] In addition, because the WGM spectrum of a typical microresonator is rather dense, it is also possible to have coresonant copropagating modes in a single resonator, either by coincidence or through strain tuning of the WGMs. In this way, crossing[5] and anticrossing[6,7] have been observed in otherwise unmodified microresonators. This is of practical as well as fundamental interest, because it means that many applications that were thought to require coupled resonators might be possible with a single resonator.[7]

This is also true of induced transparency and absorption. Whispering-gallery microresonators have two orthogonally polarized families of modes, TE (transverse electric) and TM (transverse magnetic). Because the birefringence induced by strain tuning causes the two types of modes to tune at different rates, strain tuning can be used to impose frequency degeneracy between a TE mode and a TM mode, i.e., to bring these copropagating modes into coresonance. We have noted that when this coresonance occurs, cross-polarization coupling can be observed. Because of the similarity of this coupling of coresonant orthogonally polarized modes in a single resonator to the inter-resonator coupling of coresonant modes of the same polarization, we have shown that behavior analogous to CRIT and CRIA, which we call CMIT and CMIA, for coupled-mode induced transparency and absorption, is possible.[8]

*atr@okstate.edu; phone 1 405 744-6742; fax 1 405 744-6811; physics.okstate.edu/rosenber/index.html

Advances in Slow and Fast Light VII, edited by Selim M. Shahriar, Frank A. Narducci, Proc. of SPIE
Vol. 8998, 899813 · © 2014 SPIE · CCC code: 0277-786X/14/$18 · doi: 10.1117/12.2047532

In the case of CMIT and CMIA, the light incident on the microresonator is typically linearly polarized so as to directly excite only one family of modes, say TE, and the mode coupling effects are observed as a splitting or modification of the shape of the resonant TE throughput dip (TM output is also produced). However, we discovered that if the incident light is linearly polarized at 45° (for example) in the TE-TM basis to drive coresonant modes of the two polarizations, analogous effects can be observed in the throughput of the same linear polarization as the incident light. This occurs even in the absence of cross-polarization mode coupling, demonstrating that mode superposition is sufficient to produce induced transparency and absorption. These will be referred to as coresonant polarization induced transparency and absorption (CPIT, CPIA).[8]

For the single-resonator induced transparency and absorption (CMIT and CMIA or CPIT and CPIA), the pulse delay or advancement can be enhanced by taking advantage of the multimode capability of the tapered-fiber coupler, an advantage that is not available to free-space-beam-driven ring resonators. The tapered-fiber coupler is fabricated by heating and stretching single-mode fiber to a final diameter of about 3 μm. The thinned fiber, guiding light by total internal reflection at the silica-air interface, is no longer single-mode. If the down-taper is not gradual enough to be adiabatic, some light will be transferred from the core of the single-mode fiber into multiple modes of the thinned fiber in the coupling region. These modes (assume only two carry significant power) have the same frequency but different propagation constants, so their relative phase at the coupling point can be varied by moving the microresonator longitudinally along the fiber. If the up-taper is adiabatic, only the fundamental mode of the thinned fiber will contribute to the throughput signal; the interference of the two fiber modes in exciting a single WGM can significantly change the shape of the usual throughput dip,[9,10] and the effect on IT and IA behavior can be even stronger. A simple numerical model has been used to evaluate some of these effects; the model and some results will now be described.

2. MODEL

The experimental system to be modeled is shown in the simplified generic sketch of Fig. 1. Light from a tunable laser is coupled into the WGMs of a microresonator from a tapered fiber tangent to the equatorial plane of the resonator. The input polarization is set to any desired state by a polarization controller, and the throughput is sent through a polarizing beamsplitter and the two orthogonal components are detected; the detection system can be rotated about the fiber axis.

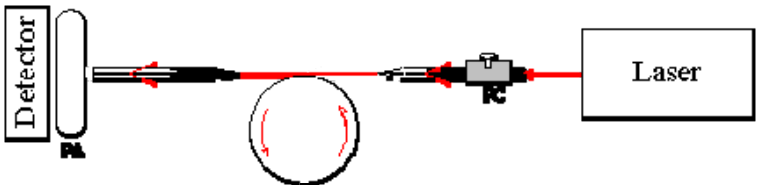

Figure 1. Whispering-gallery microresonator system for investigating induced transparency and absorption effects. The laser is tunable; PC is a polarization controller; PA is a polarization analyzer; and the detector represents an array of two detectors for measuring the powers in two orthogonal polarizations.

The model is adapted from one used previously.[8,11] After choosing the microresonator radius and the wavelength of the incident light, the polarization state of the input field may be set as desired in the TE-TM basis of the microresonator (TE is normal to the plane of Fig. 1, and TM is in the plane). The output field is resolved into orthogonal linearly polarized components, and the detection basis may be set at any angle with respect to the resonator basis. The output of the model consists of the power spectra of the two throughput components, the phase of each throughput component with respect to the input field, and the throughput pulse components when the input is a Gaussian pulse of full width at half maximum equal to $0.441/\Delta\nu_{\min}$, where $\Delta\nu_{\min}$ is the linewidth of the higher-Q mode, so that the pulse bandwidth equals the linewidth of the higher-Q mode. The resonator has two modes (TE and TM), nominally coresonant, but with a frequency detuning that can be adjusted. The two orthogonal WGMs may have different propagation constants (or effective indices of refraction), but because the input/output coupling takes place at a single point, this difference has a negligible effect on the throughput. (The model also calculates the drop signal's polarization components – which would be coupled out via another tapered fiber on the other side of the microresonator – where the difference in refractive indices of the WGMs plays a large role. The drop signal components and the throughput component orthogonal to the input will not be presented here.) The input/output coupling strengths and the cross-polarization coupling strength are determined by spatial mode overlap in an experiment; in the model, these coupling strengths are treated as adjustable parameters. Each

mode has two losses, the output coupling and intrinsic loss; these are parameters in the model, adjusted indirectly by giving the values (in the absence of cross-polarization coupling) of the quality factor Q of each mode (determines total loss), of the depth of each mode's resonance dip (determines ratio of losses), and of the coupling regime (allows determination of each loss independently). The coupling regimes are overcoupled (coupling loss greater), undercoupled (intrinsic loss greater), and critically coupled (losses equal).

Cross-polarization coupling between the intracavity circulating TE and TM modes is treated as a cross-polarization scattering near the input/output coupling point.[12] The actual cross-polarization coupling process may be due to polarization rotation of the circulating light, due, for example, to a north-south asymmetry of the slightly prolate spheroidal microresonator. However, there is almost no difference between our treatment of cross-polarization coupling and an existing model for polarization rotation in a resonator.[13,14] Our model has a scattering probability (per round trip) parameter that can be adjusted, or turned off to eliminate cross-polarization coupling.

Finally, the model allows for adjustment of properties pertaining to the two fiber modes (HE_{11} and HE_{12}, for example). These include their phase difference at the coupling point, the relative power in the higher-order mode, and the coupling strengths of the higher-order fiber mode to the two WGMs (TE and TM).

3. RESULTS

Some typical results from the model are presented in this section. In all cases, the parameter values chosen are experimentally realistic. Experimental observations of cross-polarization coupling have shown that a typical coupling strength (effective scattering probability per round trip) is a few times 10^{-8}; this is at least an order of magnitude larger than a typical backscattering strength; also, Q values of a few times 10^8 are routinely achievable in some WGMs of a fused-silica microsphere. In all of the results reported here, the TE and TM modes are assumed to be coresonant; they are labeled 1 and 2, where 1 can be TE or TM and 2 is the other. In all cases $Q_1 << Q_2$, the wavelength is taken to be 1550 nm, and the microresonator radius is 300 μm. Each of Figs. 2-4 consists of six parts: (a) and (d) show the throughput spectrum (of the same polarization component as the input), (b) and (e) give the dispersion, specifically the phase of the throughput relative to the input, and (c) and (f) show the input pulse (actually, the throughput pulse when the band center of the input pulse is far off resonance) and the throughput pulse (when the bandwidth of the input pulse is centered at the resonant frequency).

3.1 CMIT

In this case (Fig. 2), the input light is polarized along the 1 axis, so that mode 1 is driven and mode 2 is excited only by cross-polarization coupling. All parts of the figure pertain to the throughput of mode 1's polarization. Mode 1 is overcoupled, mode 2 is undercoupled. The quality factors of the two modes in the absence of cross-polarization coupling are $Q_1 = 8\times10^6$, $Q_2 = 1.98\times10^8$. The fractional dip depths of the two modes in the absence of cross-polarization coupling are $M_1 = 0.96$, $M_2 = 0.93$. The cross-polarization coupling strength is $T_s = 5\times10^{-8}$.

CMIT when driven by input light on a single fiber mode (the fundamental mode) is shown in Fig. 2(a-c). Because the transparency feature doesn't come all the way back up to 1.0, the delayed throughput pulse is attenuated; it is also broadened somewhat, indicating that the region of high dispersion is somewhat narrower than the linewidth of mode 2.

For Fig. 2(d-f), the input light is on two fiber modes; the higher-order mode has almost the same power as the fundamental mode (98%). The coupling strength of the higher-order mode to WGMs 1 and 2 is half that of the fundamental mode, and the two fiber modes are in phase at the coupling point. Comparing Figs. 2(a) and 2(d) shows a dramatic change in the throughput spectrum; the feature no longer looks like induced transparency. The dispersion on resonance in Fig. 2(e) is greater than in Fig. 2(b), and so the throughput pulse in Fig. 2(f) is delayed by more than twice as much as that in Fig. 2(c). The throughput pulse of Fig. 2(f) is somewhat more attenuated than that of Fig. 2(c), but the broadening is less.

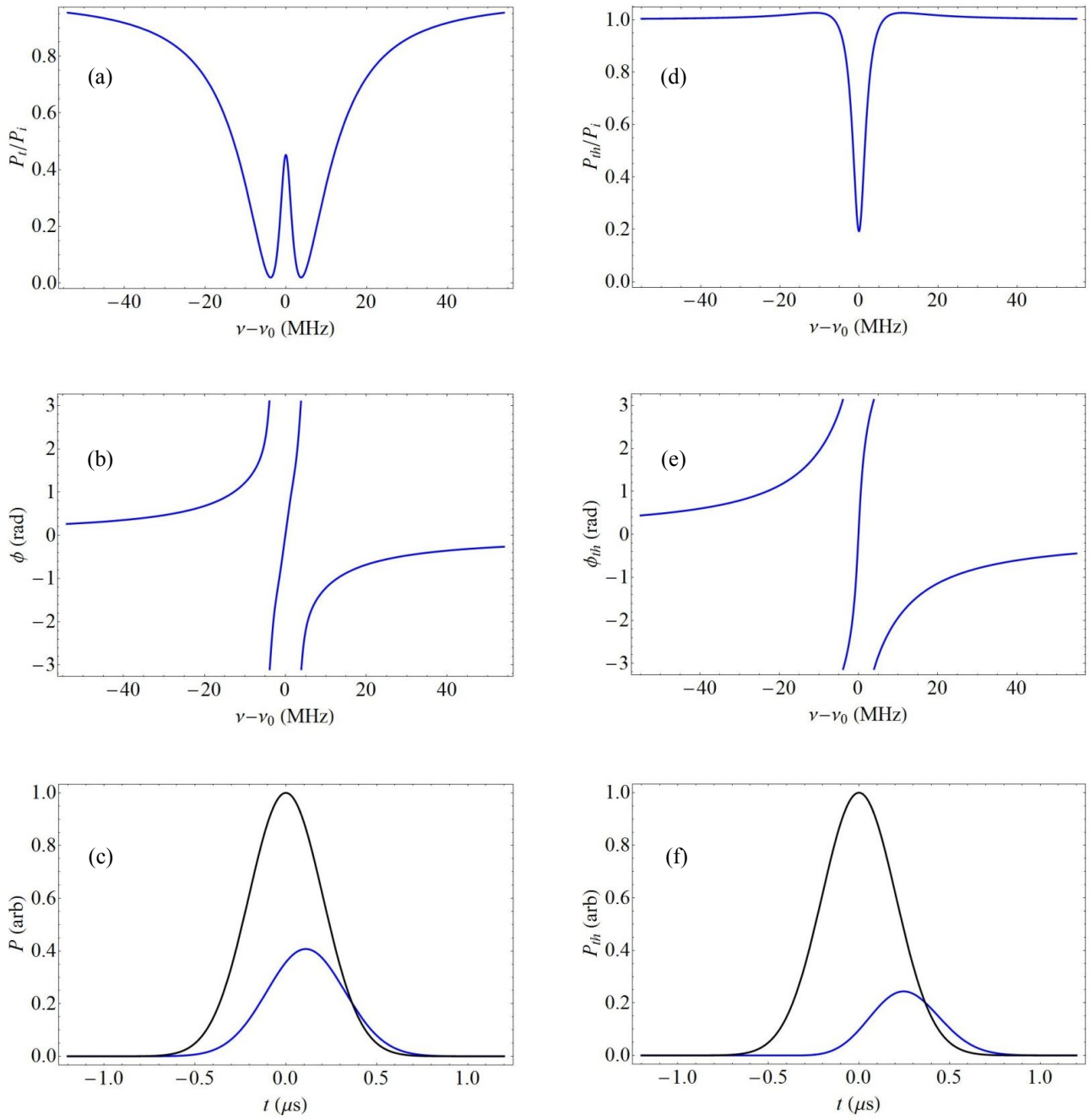

Figure 2. Coupled-mode induced transparency. (a) and (d): Throughput spectrum of the input polarization component, driving mode 1. (b) and (e): Phase shift of the throughput field relative to the input field. (c) and (f): Gaussian pulse throughput far off resonance (amplitude 1, centered at $t = 0$), and throughput pulse on resonance. For the results on the left (a-c), the input light is on the fundamental fiber mode only. For the results on the right (d-f), the input light is on both the fundamental and one higher-order fiber mode. For (d-f), the following ratios (higher-order to fundamental) are assumed: power, 0.98; strength of coupling to WGM 1, 0.50; strength of coupling to WGM 2, 0.50. The fundamental and higher-order modes are in phase at the coupling point.

3.2 CPIT/CPIA

In these examples, the input light is linearly polarized at 45°, so that both WGMs are driven with equal input power. The throughput in Figs. 3-4 is the same polarization as the input, specifically, a symmetric linear superposition of the WGMs' throughput fields. In both figures, $Q_1 = 5\times10^6$ and $Q_2 = 1\times10^8$. In contrast to the conditions of Section 3.1, there is no cross-polarization coupling in Figs. 3 and 4. For the coresonant polarization induced transparency shown in Fig. 3(a-c) and for the behavior shown in Fig. 4, both modes are overcoupled, and $M_1 = M_2 = 0.05$. The example of coresonant polarization induced absorption of Fig. 3(d-f) has both modes undercoupled and $M_1 = 0.31$, $M_2 = 0.72$.

The CPIT and CPIA responses shown in Fig. 3 are with the input light on the fundamental fiber mode only. The spectral responses of Figs. 3(a) and 3(d) show typical induced transparency and induced absorption features, respectively, and the corresponding dispersions are normal in Fig. 3(b) and anomalous in Fig. 3(e), with corresponding pulse delay in Fig. 3(c) and advancement in Fig. 3(f). These are provided as references for what can be achieved with single fiber-mode excitation.

With excitation provided by input light on both fundamental and higher-order fiber modes, pulse delay and advancement can both be achieved under the conditions for CPIT. The WGM Q values and coupling strengths in Fig. 4 are the same as in Fig. 3(a-c).

When the input power on the higher-order fiber mode is 38% that of the fundamental, the coupling strengths of the higher-order mode to the WGMs are half those of the fundamental mode, and the fiber modes are π out of phase at the coupling point, the response of Fig. 4(a-c) is produced. There is a deep throughput dip with a slight induced transparency feature, steep normal dispersion, and pulse delay. The delayed pulse of Fig. 4(c) is more attenuated than that of Fig. 3(c), but it is not as broad, and the delay is about 50% greater.

Figure 4(d-f) demonstrates how two-mode excitation can enhance the pulse advancement while simultaneously reducing its attenuation. In this case, the higher-order fiber mode carries 60% more power than the fundamental, the coupling of the higher-order fiber mode to WGM 1 is 76% as large as for the fundamental, the coupling of the higher-order fiber mode to WGM 2 is only 2% as large as for the fundamental, and the fiber modes are π out of phase at the coupling point. The throughput pulse of Fig. 4(f) is less attenuated, narrower, and advanced by nearly twice as much as in Fig. 3(f).

4. DISCUSSION

With cross-polarization coupling and fundamental fiber mode input only, an induced transparency feature is observable (CMIT, Fig. 2(a-c)). When the input is on both fundamental and higher-order fiber modes, the throughput spectrum looks different in character, but the pulse delay is enhanced. In Fig. 2(c) the delay-bandwidth product is about 0.1, but in Fig. 2(f) the delay-bandwidth product has increased to approximately 0.22.

Surprisingly, in the absence of any (cross-polarization) mode coupling, the induced transparency and absorption that may be observed with fundamental fiber mode input only (CPIT and CPIA, Fig. 3) are better than with mode coupling. The throughput at the center of the transparency feature can approach 100%, the dispersion is large, and so the throughput pulse, though somewhat attenuated and broadened, exhibits a delay-bandwidth product of about 0.3 (in Fig. 3(c)). For this case, it is easy to calculate the theoretical maximum delay-bandwidth product, which is 0.318, so the parameters of Fig. 3(a-c) are nearly optimal. The pulse advancement that is achievable in CPIA (Fig. 3(f)) is always less than the corresponding CPIT-related pulse delay. The advancement-bandwidth product is only about 0.05, and the reduced throughput due to induced absorption always means significant pulse attenuation.

However, these effects can be enhanced by using input on both fundamental and higher-order fiber modes, as seen in Fig. 4, where the CPIT resonator parameters of Fig. 3(a-c) have been used. In one case (Fig. 4(c)), the pulse delay has been increased to give a delay-bandwidth product of about 0.45, significantly better than the best that could be achieved with single-fiber-mode input. For slightly different conditions, (Fig. 4(f)), the pulse advancement has been increased to give an advancement-bandwidth product of nearly 0.1. In addition, the pulse's amplitude is hardly attenuated, thanks to the reshaping of the throughput spectrum (Fig. 4(d)).

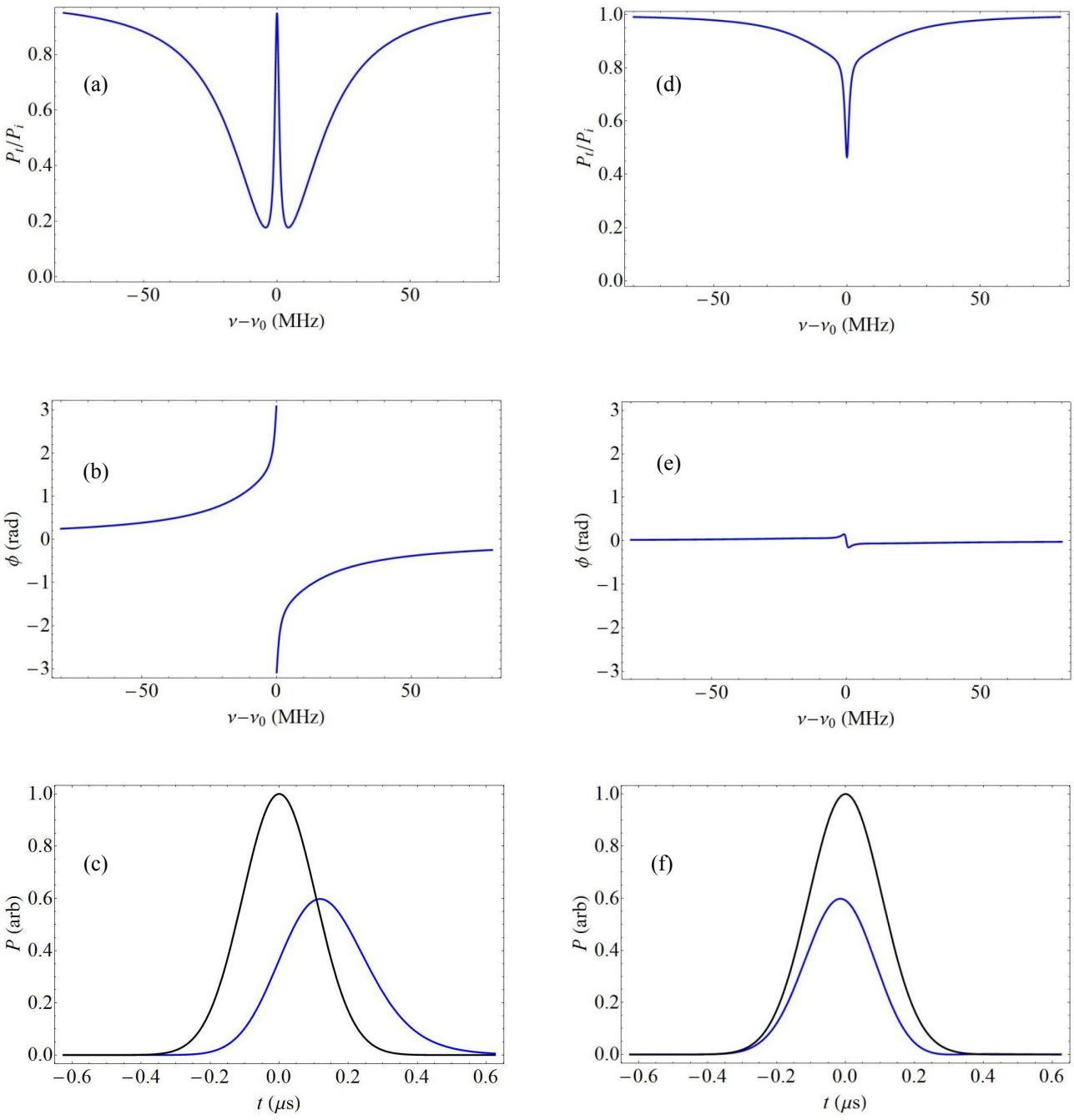

Figure 3. Coresonant polarization induced transparency (a-c) and absorption (d-f). (a) and (d): Throughput spectrum of the input polarization component at 45º, driving both modes. (b) and (e): Phase shift of the throughput field relative to the input field. (c) and (f): Gaussian pulse throughput far off resonance (amplitude 1, centered at t = 0), and throughput pulse on resonance. For all parts of this figure, the input light is on the fundamental fiber mode only.

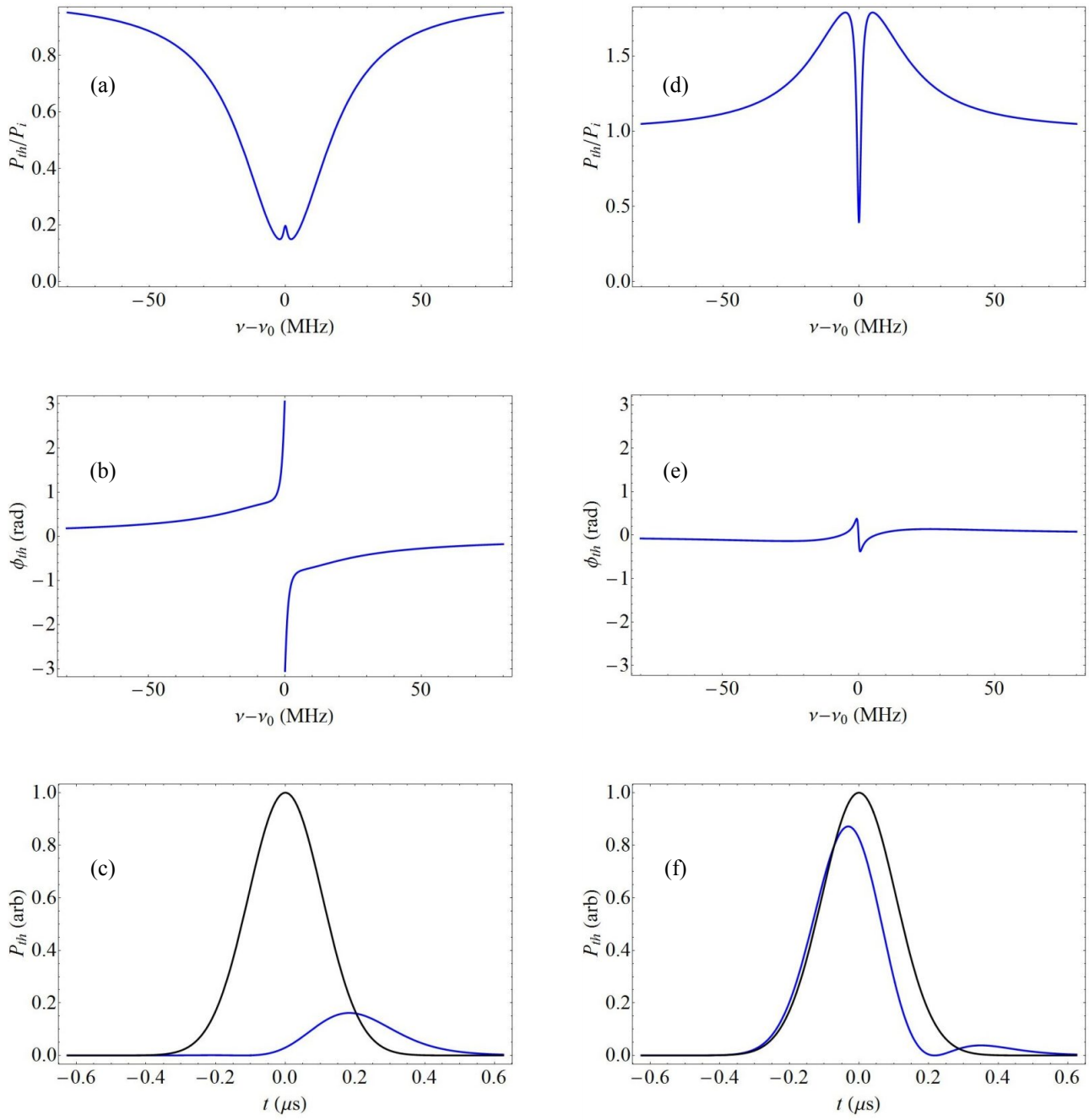

Figure 4. Coresonant polarization induced transparency conditions with two-mode excitation. (a) and (d): Throughput spectrum of the input polarization component at 45º, driving both modes. (b) and (e): Phase shift of the throughput field relative to the input field. (c) and (f): Gaussian pulse throughput far off resonance (amplitude 1, centered at t = 0), and throughput pulse on resonance. For the results on the left (a-c), the following ratios (higher-order to fundamental) are assumed: power, 0.38; strength of coupling to WGM 1, 0.50; strength of coupling to WGM 2, 0.50. For (d-f), the following ratios (higher-order to fundamental) are assumed: power, 1.6; strength of coupling to WGM 1, 0.76; strength of coupling to WGM 2, 0.02. In both cases, the fundamental and higher-order modes are π out of phase at the coupling point.

5. CONCLUSIONS

Induced transparency and absorption effects, specifically pulse delay and advancement, using a single resonator that has coresonant TE and TM whispering-gallery modes, not only with but also without cross-polarization mode coupling, can be enhanced through the use of two-fiber-mode excitation. The effects reported here might be useful for application in areas such as chemical sensing, either absorption sensing or dispersion sensing through frequency shifts. Experimental studies of CM/CP IT and IA, including pulse response, have confirmed the predicted behavior with single-fiber-mode excitation, and two-fiber-mode excitation studies, using asymmetrically tapered coupling fibers, are planned. The use of hollow-bottle microresonators for these experiments is underway, and promises to allow much more flexibility in the variation of experimental parameters.

ACKNOWLEDGMENTS

The author would like to thank his current and former graduate students who contributed to this work, especially to the experimental observation and study of some of the effects described here. Particular thanks go to Elijah Dale, Erik Gonzales, and Khoa Bui; others more peripherally involved include Jeromy Rezac, George Farca, Siyka Shopova, Deepak Ganta, Gregorio Martinez, and Razvan Stoian. Some initial aspects of this work were made possible by support from the National Science Foundation through Grant Number ECCS-0601362, and from the Oklahoma Center for the Advancement of Science and Technology through Grant Number AR072-066.

REFERENCES

[1] Fleischhauer, M., Imamoglu, A., and Marangos, J. P., "Electromagnetically induced transparency: Optics in coherent media," Rev. Mod. Phys. 77, 633-673 (2005).
[2] Smith, D. D., Chang, H., Fuller, K. A., Rosenberger, A. T., and Boyd, R. W., "Coupled-resonator-induced transparency," Phys. Rev. A. 69, 063804 (2004).
[3] Naweed, A., Farca, G., Shopova, S. I., and Rosenberger, A. T., "Induced Transparency and Absorption in Coupled Whispering-Gallery Microresonators," Phys. Rev. A 71, 043804 (2005).
[4] Kippenberg, T. J., Spillane, S. M., and Vahala, K. J., "Modal coupling in traveling-wave resonators," Opt. Lett. 27, 1669-1671 (2002).
[5] Savchenkov, A. A., Matsko, A. B., Ilchenko, V. S., Strekalov, D., and Maleki, L., "Direct observation of stopped light in a whispering-gallery-mode microresonator," Phys. Rev. A 76, 023816 (2007).
[6] von Klitzing, W., Long, R., Ilchenko, V. S., Hare, J., and Lefèvre-Seguin, V., "Tunable whispering gallery modes for spectroscopy and CQED experiments," New Journal of Physics 3, 14.1-14.14 (2001).
[7] Carmon, T., Schwefel, H. G. L., Yang, L., Oxborrow, M., Stone, A. D., and Vahala, K. J., "Static Envelope Patterns in Composite Resonances Generated by Level Crossing in Optical Toroidal Microcavities," Phys. Rev. Lett. 100, 103905 (2008).
[8] Rosenberger, A. T., "EIT analogs using orthogonally polarized modes of a single whispering-gallery microresonator," Proc. SPIE 8636, 863602-1—863602-11 (2013).
[9] Chiba, A., Fujiwara, H., Hotta, J., Takeuchi, S., and Sasaki, K., "Fano resonance in a multimode tapered fiber coupled with a microspherical cavity," Appl. Phys. Lett. 86, 261106 (2005).
[10] Ruege, A. C. and Reano, R. M., "Multimode Waveguides Coupled to Single Mode Ring Resonators," J. Lightwave Technol. 27, 2035-2043 (2009).
[11] Rosenberger, A. T., "Analysis of whispering-gallery microcavity-enhanced chemical absorption sensors," Opt. Express 15, 12959-12964 (2007).
[12] Rubin, J. T., and Deych, L., "*Ab initio* theory of defect scattering in spherical whispering-gallery-mode microresonators," Phys. Rev. A 81, 053827 (2010).
[13] Melloni, A., Morichetti, F., and Martinelli, M., "Polarization conversion in ring resonator phase shifters," Opt. Lett. 29, 2785-2787 (2004).
[14] Morichetti, F., Melloni, A., and Martinelli, M., "Effects of Polarization Rotation in Optical Ring-Resonator-Based Devices," J. Lightwave Technol. 24, 573-585 (2006).